

See discussions, stats, and author profiles for this publication at: <https://www.researchgate.net/publication/41426071>

100% Efficient Sub-Nanoliter Sample Introduction in Laser-Induced Breakdown Spectroscopy and Inductively Coupled Plasma Spectrometry: Implications for Ultralow Sample Volumes

ARTICLE in ANALYTICAL CHEMISTRY · FEBRUARY 2010

Impact Factor: 5.64 · DOI: 10.1021/ac901966z · Source: PubMed

CITATIONS

27

READS

33

6 AUTHORS, INCLUDING:



Sebastian Groh

Technische Universität Dortmund

12 PUBLICATIONS 234 CITATIONS

SEE PROFILE



Praseon Diwakar

Purdue University

40 PUBLICATIONS 422 CITATIONS

SEE PROFILE



Carmen Cecilia Garcia

Karlsruhe Institute of Technology

23 PUBLICATIONS 640 CITATIONS

SEE PROFILE



David W Hahn

University of Florida

114 PUBLICATIONS 2,574 CITATIONS

SEE PROFILE

100% Efficient Sub-Nanoliter Sample Introduction in Laser-Induced Breakdown Spectroscopy and Inductively Coupled Plasma Spectrometry: Implications for Ultralow Sample Volumes

S. Groh,[†] P. K. Diwakar,[‡] C. C. Garcia,[†] A. Murtazin,[†] D. W. Hahn,^{*,‡} and K. Niemax[†]

Plasma-Analyte Interaction Working Group (PAIWG), Department of Mechanical & Aerospace Engineering, University of Florida, Gainesville, Florida 32611, and ISAS-Institute for Analytical Sciences at Technische Universität Dortmund, Germany

Recently, nanoflow nebulizers with low-volume drain-free spray chambers became available for inductively coupled plasma-mass spectrometry application for analysis of very small sampling volumes. The present technical note reports on a different approach for 100% efficient sub-nanoliter sample introduction, the application of mono-disperse piezoelectric microdroplet dispensers which generate 40–50 μm droplets with high reproducibility if nozzles of 30 μm diameter are applied. The droplets having volumes below 0.1 nL can be introduced loss-free and without plasma loading, with frequencies up to ~ 100 Hz into analytical plasmas. In this technical note, the analytical figures of merit of laser-induced breakdown spectroscopy and inductively coupled plasma-optical emission spectrometry with single droplet introduction are reported using Ca and Au standard solutions as examples. Future engineering is required to reduce the total sample volumes from the relatively large sample reservoir of the current study, thereby reducing potential issues of wash-out while enabling analysis of ultralow total sample volumes.

There is an increasing demand in analytical chemistry to develop techniques for the analysis of very small sample volumes. In particular, in bioanalytical chemistry sample volumes may be very limited.¹ There are several other situations that can lead to limited availability of sample, including biological experiments, forensics, clinical chemistry, toxicology, experiments involving radioactive analytes, and speciation analysis. Collection of samples in the range of 10–50 nL is very common in the above-mentioned fields, and reliable techniques for the introduction of the sample analyte are required.² Increasing the volume of sample by diluting can be a part of the solution, but this can lead to issues of sensitivity and detection limits.

Complete characterization of a biochemical compound involves detection of the elemental species, structure of the compound,

oxidation state of various elements, and chemical form of various elements in the compound, which altogether determine the biological, chemical, and toxic properties of the compound. For such an analysis, a combination of two or more analytical techniques is required. One which can perform speciation or species separation and another that can detect and quantify the elemental composition of the compound. Nanohigh-performance liquid chromatography (nano-HPLC) has become a widely used speciation technique in various applications including proteomics, toxicology, and biological studies. The main advantages of nano-HPLC include low sample consumption, rapid analysis, improved separation efficiency, and reduced waste generation, adsorptions, and sample dilution effects. Usually, nano-HPLC is coupled with the electrospray ionization (ESI) MS/MS technique for molecular structure characterization, but ESI MS/MS is compound-dependent and suffers heavily from matrix effects and thereby absolute quantification is often not possible. Also, ESI (MS/MS) cannot provide elemental information, which calls for the need of an analytical technique which is truly a multielement detection technique and can be effectively coupled with nano-HPLC for quantitative analysis. Inductively coupled plasma mass spectrometry (ICPMS) and, if a somewhat lower detection power is sufficient, laser-induced breakdown spectroscopy (LIBS) are excellent candidates for elemental detection and quantification. ICPMS offers excellent sensitivity, low matrix effects, and high dynamic range, while LIBS offers good sensitivity and reduced experimental complexity for elemental detection which can be useful in certain applications. The major challenge in coupling nano-HPLC with ICPMS and LIBS is the sample flow rate incompatibilities between the HPLC column flow rates and ICP/LIBS nebulizer flow rates. Sensitivity of ICPMS is severely diminished due to low flow rates from HPLC columns. Recently, significant progress has been reported in hyphenation of nano-HPLC and ICPMS, introducing nanoflow nebulizers with low-volume drain-free spray chambers.^{3–5} For example, applying nanovolume flow injection, 54 nL samples spiked with U and Pu

* To whom correspondence should be addressed. E-mail: dwhahn@ufl.edu.

[†] ISAS-Institute for Analytical Sciences at Technische Universität Dortmund.

[‡] University of Florida.

(1) Manz, A.; Pamme, N.; Iossifidis, D. *Bioanalytical Chemistry*; Imperial College Press: London, U.K., 2003.

(2) Todoli, J. L.; Mermet, J. M. *Spectrochim. Acta, Part B* 2006, 61, 239.

(3) Schaumlöffel, D.; Giusti, P.; Zoriy, M. V.; Pickhardt, C.; Szpunar, J.; Lobinski, R.; Becker, J. S. *J. Anal. At. Spectrom.* 2005, 20, 17.

(4) Giusti, P.; Lobinski, R.; Szpunar, J.; Schaumlöffel, D. *Anal. Chem.* 2007, 79, 965.

(5) Brennan, R. G.; Murdock, S. A. E. O.; Farmand, M.; Kahen, K.; Samii, S.; Gray, J. M.; Montaser, A. *J. Anal. At. Spectrom.* 2007, 22, 1199.

were injected into the continuous flow of a buffer at $7 \mu\text{L min}^{-1}$ and finally introduced into an ICPMS.³ The authors quoted impressive detection power of the experimental arrangement for nano-HPLC-ICPMS. Relative detection limits of 1.6×10^{-12} and $0.3 \times 10^{-12} \text{ g mL}^{-1}$ and absolute detection limits of 9.1×10^{-17} and $1.5 \times 10^{-17} \text{ g}$ were quoted for ^{238}U and ^{243}Am , respectively. Giusti et al. have reported improved figures of merit by using nanoflow nebulizers as compared with microflow nebulizers for selenium-containing peptide quantification studies.⁶ By introducing nanoliter range sample volumes, they obtained stable sample introduction resulting in accurate and sensitive detection in the nanoliter volume range. Absolute detection limits for Se in the femtogram range were achieved. In order to obtain better figures of merit and 100% transport efficiency and low sample consumption, direct injection nebulizers can provide better results. Brennan et al. studied analytical performance of a direct injection high-efficiency nebulizer (d-DIHEN) at low solution flow rates using nanoliter sample volume injection.⁵ They obtained improved stability in sample introduction and As detection limits in the picogram range, similar or better as compared with a high solution uptake based nano-HPLC coupled ICPMS system. Schaumloffel et al. obtained a detection limit for sulfur in the femtogram range ($45 \mu\text{g/L}$) using the nano-HPLC-ICPMS technique.³

Our strategy is different. We propose discontinuous sample introduction into the plasma by monodisperse microdroplets (MDMD). With application of, for example, $30 \mu\text{m}$ orifices, droplets of $40\text{--}50 \mu\text{m}$ in diameter can be produced from a solution. Note that the sample volume of such droplets is between 33 and 65 pL, which is about 3 orders of magnitude less than in the nano-HPLC-ICPMS experiment mentioned above. The total volume introduced by MDMD can vary from a single droplet up to 1000 times the droplet volume per second if droplet frequencies up to 1000 Hz are applied. Subnanoliter range analyte introduction to the plasma can have an advantageous effect, as the plasma cooling will be limited to localized regions as compared to the analyte introduction using a nebulizer, where heavy mass loading can lead to overall plasma cooling and thereby interfere with the LIBS or ICPMS signal. A liquid droplet containing low volumes of analyte can address the above-mentioned issues pertaining to small sample availability and sensitivity issues in aqueous media. A single droplet provides a better means of analysis by LIBS as the breakdown mechanism surrounding an isolated droplet is different than in direct breakdown of bulk liquids.

MDMD introduction into the ICP and the atomization of the droplet has been studied by Olesik,⁷ Lazar and Farnsworth,⁸ and more recently in the current laboratory.⁹ However, the first experiments with MDMD stem back to earlier research performed by the group of Hieftje, who used a droplet generator to study desolvation and atomization processes in analytical flames.¹⁰ Janzen et al. developed a HPLC-LIBS system using a similar MDMD sample introduction technique and obtained detection

limits in the parts per billion (ppb) range for calcium and sodium.¹¹

The present technical note is showing the analytical potential of MDMD introduction of very small samples into analytical plasmas by applying a commercial droplet dispenser which has unfortunately a relatively large dead volume for introduction of very small volumes, which can lead to large washout times and peak broadening.⁸ This means that droplet generating piezoelectric capillaries have to be directly coupled to nano-HPLC or a microfluidic separation system to minimize the dead volumes for better performance. Therefore, while the current study is limited to relatively large total sample volumes (i.e., reservoir) of the commercial dispenser, as noted below, future implementations may significantly reduce or eliminate the dead volume issue via an engineering design. Accordingly, this study will focus only on the droplet sample volume, noting that current dispenser designs may actually achieve smaller droplet volumes than the current study.

Although application of ICPMS would present the best figures of merit, the less expensive and less powerful ICP-OES detection was used. In addition, the analytical power of the very compact and even less complex detection by laser-induced breakdown spectroscopy for analysis of single droplets¹² was applied.

EXPERIMENTAL SECTION

Single Droplet Sample Introduction System. A scientific grade microdroplet dispenser system was used for generating single droplets of analyte in the size range of $40\text{--}60 \mu\text{m}$ (MD-K-150, Microdrop Technologies). Various research groups have used a similar kind of droplet generator and droplet introduction methods in analytical plasmas.^{9–11} The system consists of a dispenser head, a reservoir, and an electronic controller. The reservoir can hold about 5 mL of liquid. The dispenser system uses a piezoelectric nozzle, commonly used in ink jet printers, to generate ‘on demand’ single isolated droplets. The system uses a capillary tube, surrounded by a piezoelectric tube, which is filled with the sample liquid, and the piezoelectric is activated with a voltage pulse which sends a pressure pulse across the liquid causing liquid motion at the nozzle. The velocity of the liquid reaches several meters per second in a short time, and then it decelerates owing to the pressure loss and expansion through the nozzle. Combined with inertial forces and inertial surface tension forces, individual single droplets are formed at the nozzle propagating at a speed in the range of $1\text{--}5 \text{ m/s}$. The repetition rate can be chosen up to 2000 Hz. The size of the droplet is dependent on the nozzle diameter, viscosity of liquid, and control parameters, including the applied voltage level and pulse width. In this case, the dispenser head is also equipped with a protective gas sheath flow around the droplet orifice. Manufacturers of the system have reported reproducibility of the droplets to be very high if all the parameters are kept optimum and constant and report variability in droplet volume to be less than 1%. Several other studies using similar droplet generation systems have

(6) Giusti, P.; Schaumloffel, D.; Encinar, J. R.; Szpunar, J. J. *Anal. At. Spectrom.* **2005**, *20*, 1101.

(7) Olesik, J. W. *Appl. Spectrosc.* **1997**, *51*, A158.

(8) Lazar, A. C.; Farnsworth, P. B. *Appl. Spectrosc.* **1997**, *51*, 617.

(9) Groh, S.; Garcia, C. C.; Murtazin, A.; Horvatic, V.; Niemax, K. *Spectrochim. Acta, Part B* **2009**, *64*, 247.

(10) Russo, R. E.; Withnell, R.; Hieftje, G. M. *Appl. Spectrosc.* **1981**, *35*, 531.

(11) Janzen, C.; Fleige, R.; Noll, R.; Schwenke, H.; Lahmann, W.; Knoth, J.; Beaven, P.; Jantzen, E.; Oest, A.; Koke, P. *Spectrochim. Acta, Part B* **2005**, *60*, 993.

(12) Hahn, D. W.; Lunden, M. M. *Aerosol Sci. Technol.* **2000**, *33*, 30.

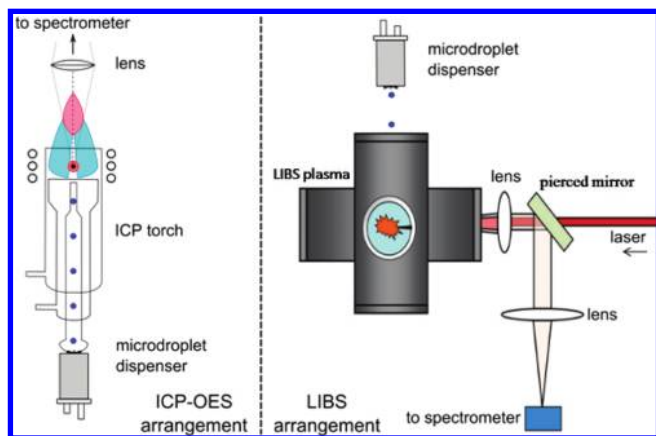


Figure 1. Experimental arrangements for inductively coupled plasma experiments (left) and laser-induced plasma experiments (right).

reported variability to be in range of less than 1–5%.^{13,14} The droplet generation process can be triggered internally, externally, or manually. Strobe light arrangement is used for visualizing the droplet formation at the nozzle, where the delay of the stroboscope ranges from 0 to 900 μ s. In the current study, a 30 μ m nozzle diameter is used for generating the single isolated droplets. The resulting droplets are in range from 40 to 60 μ m with an exit velocity ranging between 1.5 and 4 m/s. All the LIBS experiments in the current study were performed with a droplet size of 50 μ m, which is equivalent to an analyte volume of 65 pL. Droplets were generated using the external trigger mode, wherein the flashlamp of the 1064 nm LIBS laser was used to trigger the droplet generator with a frequency of 5 Hz. Figure 1 shows experimental arrangements for ICP and LIBS experiments.

Optical Configuration and Data Collection. The vertically positioned ICP was operated in argon with a high frequency power of 1000 W and an auxiliary and outer Ar flow of 1 and 16 L/min, respectively. The emitted light was collected end-on using quartz lenses and a multifurcated optical fiber bundle and imaged onto the entrance slits of a Jobin-Yvon SPEX 1000 M monochromator with a focal length of 1 m and a McPherson EU700 monochromator with a focal length of 0.3 m. The SPEX monochromator was used for observation of the analyte element emission lines, while the EU700 model was used to simultaneously observe the emission on the 486.13 nm hydrogen line as an indicator for the presence of droplets in the plasma in the case of very small or no visible analyte signal due to low concentrations. Both monochromators were equipped with EMI 9789QA photomultipliers. The photomultiplier signals were amplified by a Stanford Research Systems SR570 amplifier (SPEX) and a Keithley 428 amplifier (EU700) and recorded using a digital-analog-converter (National Instruments DAQPad-6015) connected to a personal computer. More detailed information about the optical setup and methods of data acquisition is given in a previous publication.⁹

The single droplets with diameters of 49–53 μ m (according to a volume of 62–78 pL) and an initial velocity of 3.1–3.9 m/s were introduced into the plasma by attaching the microdroplet dispenser head directly to the injector tube of the ICP torch. They

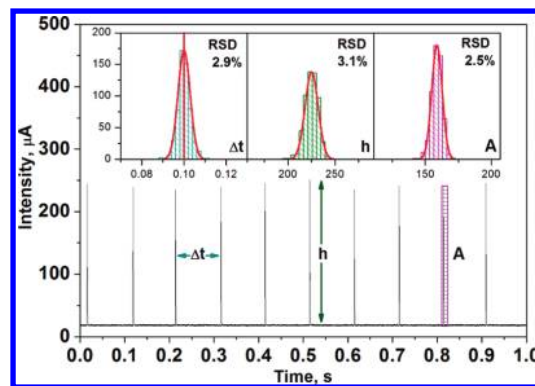


Figure 2. Signal waveforms and peak statistics for calcium standard solution ([Ca] = 1 μ g/mL, Ca II 393.36 nm, flow rate 0.206 L/min, plasma power 1.0 kW, droplet frequency 10 Hz).

Table 1. Droplet Generator Parameters

droplet generator model	MD-K-150
nozzle diameter	30 μ m
connecting tube	PTFE
driver voltage	70–90 V
pulse length	40–50 μ s
drop speed	1.5–2 m/s
droplet diameter	50 μ m
repetition rate	5 Hz (LIBS), 10 Hz (ICP-OES)

were transported upward along the tube by means of an argon gas flow of 0.2 L/min from the protective gas sheath around the droplet orifice. Note that this transport gas flow instead of the initial droplet velocity has the foremost influence on the transport time through the injector tube. Together with the transport gas flow, the initial velocity of the droplets, however, has significant influence on the stability of the droplet transport. With the above-mentioned parameters, stability was obtained for the conditions presented in Figure 2 and Table 1. The distributions of the length of the time interval between two emission peaks, the peak height, and the peak area are shown therein.

For the LIBS experiments, an Nd:YAG pulsed laser operating at its fundamental wavelength (1064 nm, 5 ns fwhm, 5 Hz, 315 mJ/pulse) was used for creating the laser-induced plasma. A second Nd:YAG laser operating at 532 nm (5 ns fwhm, 5 Hz, 15 mJ) was used for droplet imaging/visualization and droplet alignment in the LIBS plasma. Figure 1 shows the schematic of the LIBS experimental setup. The LIBS laser is focused onto the center of the six-way cross using a 100 mm focal-length, UV-grade condensing lens. The imaging laser beam is configured coaxial to the LIBS laser beam such that it crosses the exact focal volume of the LIBS plasma. Plasma emission is collected by employing backscattering geometry using a pierced mirror, and the subsequent signal is fiber coupled to a 0.3 m spectrometer and recorded using an intensified charge-coupled device (ICCD) camera. Plasma imaging was accomplished using a UV-grade achromatic lens and a second ICCD camera arranged orthogonal to the 1064 nm laser beam. Single droplets of size 50 μ m were introduced vertically downward from the droplet generator. The flashlamp sync of the LIBS laser was used to trigger two delay generators, which in turn triggered the 532 nm laser, the imaging ICCD camera, and the droplet generator. Timing was adjusted in such a way that the imaging laser and the ICCD could then be moved in concert relative to the LIBS laser pulse. The droplet generator timing was

(13) Jacob, P.; Stockhaus, A.; Hergenroder, R.; Klockow, D. *Fresenius' J. Anal. Chem.* **2001**, *371*, 726.

(14) Englmam, M.; Fekette, A.; Gebefugi, I.; Kopplin, P. S. *Anal. Bioanal. Chem.* **2007**, *388*, 1109.

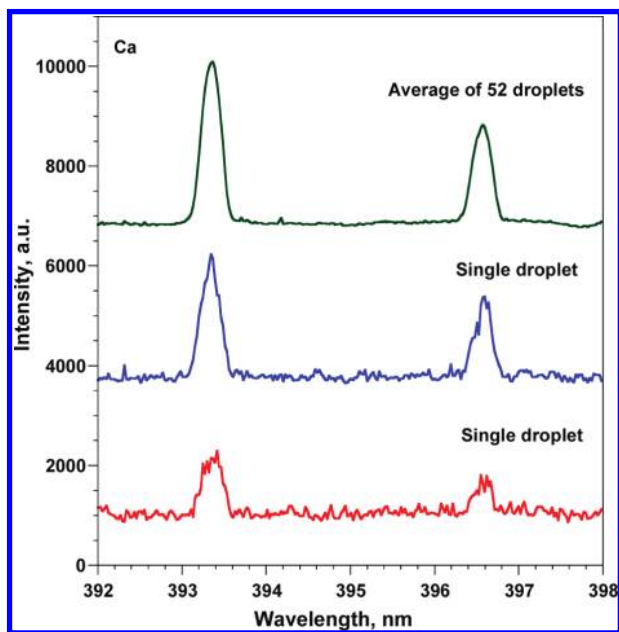


Figure 3. LIBS spectra for a calcium concentration of 1 $\mu\text{g/mL}$ corresponding to 50 μm diameter droplets. All spectra have the same intensity scale and have been shifted vertically for clarity.

adjusted such that the droplets were temporally and spatially aligned with the focal point of the LIBS laser. The plasma then formed about the droplet, breaking down the surrounding air and thereby engulfing the droplet within the ensuing plasma volume. A nitrogen flow of 0.2 L/min was used for the sheath flow about the droplet stream. The size and velocity of the droplet was measured by calibrating the nozzle diameter as observed on the monitor screen. To prevent capillary clogging, the analyte was filtered using a 0.2 μm pore membrane filter before transferring the analyte to the reservoir. In addition, regular cleaning of the capillary was done with ultrapurified deionized water and 3% HNO_3 , as needed.

RESULTS AND DISCUSSION

For both the LIBS and ICP-OES configurations, Ca and Au were used as analyte test species for obtaining calibration curves and detection limits using the single droplet analyte introduction approach. In the case of the LIBS measurements, the analyte solution was prepared by diluting ICP-grade analytical standards of 10 000 $\mu\text{g/mL}$ of Ca and 1 000 $\mu\text{g/mL}$ of Au (SPEX Certiprep). Serial dilution was used to prepare the desired concentration using ultrapurified deionized water, and stock solutions were prepared in the range of 0.5–10 $\mu\text{g/mL}$ for Ca and 100–1000 $\mu\text{g/mL}$ for Au.

For the LIBS experiments, single 50 μm droplets were generated and injected into the laser focal volume from a distance of 10 mm above the focal spot. For the calcium analyte, spectra were collected at a delay of 30 μs following plasma initiation and integrated using a 20 μs gate width. Series of spectra were recorded in sets of 100 for Ca concentrations of 0.5, 1.0, 2.5, 5.0, and 10.0 $\mu\text{g/mL}$. Representative calcium spectra are shown in Figure 3 for a concentration of 1 $\mu\text{g/mL}$. Spectral data were processed using a two-step algorithm. In the first step, the P/B ratio (integrated full-peak area normalized to adjacent continuum intensity) of the two calcium II emission peaks at 393.36 nm

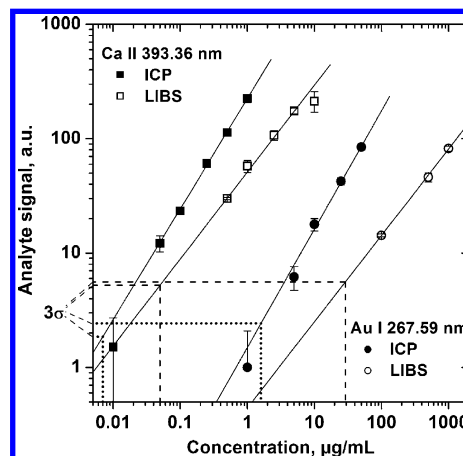


Figure 4. Calibration curves for Ca and Au, obtained for the LIBS and ICP-OES configurations. For LIBS data, the analyte signal is the P/B ratio. For ICP data, the analyte signal is the peak height in microamps. The 3σ detection limits for Ca are 7 ng/mL, corresponding to 0.5 fg/droplet (with ICP) and 0.05 $\mu\text{g/mL}$ or 23 fg/droplet (with LIBS). Detection limits for Au are 1.6 $\mu\text{g/mL}$ or 0.1 pg/droplet (with ICP) and 29 $\mu\text{g/mL}$ or 12.7 pg/droplet (with LIBS). The detection limits are marked as dotted and dashed lines for ICP-OES and LIBS, respectively.

(0–25 414 cm^{-1}) and 396.85 nm (0–25 192 cm^{-1}) was calculated, and all spectra in which the ratio of the 393.36 to 396.85 P/B signals was less than 1.1 or greater than 2.4 were rejected. In the second step, spectra with the 393.36 nm P/B value less than 10 were rejected. The remaining spectra were then averaged for each 100-shot set and used to calculate the final P/B value using the 393.97 nm Ca II line. Overall, the process was designed to remove spectra corresponding to noise rather than actual calcium emission and was refined based on the statistical study of a large number of unambiguous calcium-containing spectra. Rejected spectra are believed to correspond to individual LIBS plasmas in which the microdroplet was not sufficiently sampled by the plasma, presumably due to drifting of the falling droplet away from the primary plasma volume. This process was repeated for gold analyte solutions using concentrations from 100 to 1000 $\mu\text{g/mL}$. For the Au analysis, the P/B ratio was calculated using the 267.59 nm (0–37 359 cm^{-1}) emission line for a detector delay time of 20 μs and a 20 μs gate width. Because only one Au emission line was available in the spectral window, the data were processed by only rejecting spectra with a Au P/B ratio less than 10.

The calibration curve for the LIBS Ca and Au data is shown below in Figure 4. The detection limits were obtained applying the 3σ criterion. For Ca in the current study, it was determined to be 0.05 $\mu\text{g/mL}$. This detection limit corresponds to an average of about 50 droplets, each of 65 pL volume of Ca analyte, which corresponds to a total analyte mass of 160 fg (3.3 fg per droplet). For single droplet events, the absolute detectable mass is 23 fg per droplet when accounting for the increase in spectral noise when not averaging. The calibration curve for Au, also shown in Figure 4, was obtained for a concentration range of 100–1000 $\mu\text{g/mL}$. The corresponding detection limit was determined to be 29 $\mu\text{g/mL}$. It is important to mention here that both calibration curves are slightly biased toward higher P/B values at low concentrations due to rejection of spectra by the processing algorithm that contain actual analyte emission features that are near the detection limit.

The Ca detection limit in a similar LIBS study by Janzen et al. was reported¹¹ to be 20 ng/g which is comparable to the detection limit obtained in the current study (50 ng/g). However in contrast, the volume of droplets in Janzen's study was 280 pL as compared to 65 pL in the present work. On the basis of recent work,¹⁵ it is believed that the plasma forms about the droplet (i.e., air breakdown), subsequently vaporizing the droplet and sampling the analyte species, although allowing sufficient residence time for diffusion of heat and analyte species is important to avoid localized matrix effects.¹⁶ ICPMS and ICP-OES can achieve limits of detection in the parts per trillion and parts per billion range, respectively. Compactness (size) and cost-effectiveness (less expensive instrumentation and operation) of the LIBS approach provide an easy means of subnanoliter analyte introduction, which can be useful in analytical conditions where low analyte volume is available while the analyte concentration is not the limiting factor. In such cases, detection of absolute mass becomes the key, and the LIBS system can provide excellent results.

For the calibration with Ca and Au as analyte species using the ICP-OES instrumentation and the microdroplet dispenser, as described above, standard solutions with original concentrations of 1000 $\mu\text{g/mL}$ Ca in 5% HNO_3 and 1000 $\mu\text{g/mL}$ Au in 20% HCl , respectively, (both by Johnson Matthey GmbH) were diluted with deionized water to the desired concentrations. These covered a concentration range of 0–1.0 $\mu\text{g/mL}$ in case of Ca and 0–50 $\mu\text{g/mL}$ in the case of Au. The droplets created from the prepared solutions were introduced into the ICP with a repetition rate of 10 droplets per second, and the pulsed emission signal was recorded over a time span of about a minute. The observed emission lines were the Ca ion line at 393.36 nm and the neutral Au line at 267.59 nm. Note that these are the same emission lines used for the LIBS measurements. For the Ca measurements, the low-pass filter of the amplifier was set to a cutoff frequency of 1 kHz in order to reduce the high-frequency noise, and the data were acquired at a sampling frequency of 30 kHz. In the case of Au, the filter cutoff was set to 30 kHz and data acquisition was done with a sampling frequency of 100 kHz.

After subtraction of the background intensity, the emission peaks were extracted from the complete recorded time-dependent signal, aligned at the bottom of their rising slopes, and averaged using an algorithm programmed in MATLAB and Origin, respectively. The averaged peak intensities measured at different analyte concentrations with 500 droplets each are plotted together with the LIBS data in Figure 4. The slopes of the calibration lines are 0.97 and 1.03 for Ca and Au, respectively. The ICP-OES detection limits were also determined employing the 3σ -criterion, where σ is the standard deviation of the blank signal during droplet atomization. The detection limits were 7 ng/mL and 1.6 $\mu\text{g/mL}$ for Ca and Au, respectively (see Figure 4). These data correspond to total masses of 0.5 fg of calcium and 0.1 pg of gold per droplet if one takes into account the droplet diameter of 50 μm . These values are greater than results previously reported with a mono-disperse, dried microparticulate injector system for a different analyte, namely, a detection limit of 0.05 ng/mL for Ba.⁸ In their study, droplet desolvation was complete prior to ICP injection,

while ensemble averaging provided baseline compensation. It has to be noted that the data points near the detection limits and the blank values have large uncertainties because of a still significant influence of the evaporated water of the 50 μm droplet on the local plasma conditions and, therefore, on the line intensities.⁹ However, as also noted by Groh et al.,⁹ the introduction of smaller droplets, e.g., with diameters smaller than 40 μm , would minimize the perturbation.

There are other approaches toward the analysis of very low sample quantities. For example, the use of microconcentric nebulizers in combination with nano-HPLC allows achieving low detection limits while only consuming sample volumes in the nanoliter range for a single analysis run. Schaumlöffel et al. report detection limits of 1.6 and 0.3 pg/mL for uranium and plutonium, respectively.³ These were attained by 10-fold introduction of sample amounts of 54 nL each and subsequent averaging of the 10 resulting peaks with an individual length of about 10 s. Using the above-described MDMD setup with individual droplet volume of 60 pL, it takes the same time to introduce approximately the same sample volume when running the droplet generator with a repetition rate of 100 Hz. In that case, however, the measured signal consists of about 10 000 individual peaks instead of 10. The peak signal of each individual droplet will be higher than the quasi-continuous introduction of the larger sample volume since the integrated signals are the same, unless droplet introduction is causing overloads of the plasma. The improvement depends on the length of the droplet signals. In the particular case discussed above, the improvement would be a factor of about 10 taking into account a signal width of 1 ms. The higher number of peaks to average also has obvious statistical advantages for the signal-to-noise ratio of the measurement. The applied repetition rate of 100 Hz ensures a limited plasma loading since only a local cooling effect due to droplet evaporation occurs,⁹ while in contrast, the constant introduction of liquid sample by a nebulizer leads to a considerably strong total plasma cooling.

Note that the present work is done using ICP optical emission spectrometry. For further improvement of the detection limit it makes sense to move onto mass spectrometric measurements, which typically provides elemental detection limits which are 2–3 orders of magnitude lower. Applying the reproducible, pulsed introduction of sample the resulting signal can be considered to be modulated with the trigger frequency of the droplet generator. That might be utilized to eliminate much of the noise by employing lock-in-amplifiers.

CONCLUSIONS

In this study, an alternative sample introduction system, which provides the analysis of the smallest sample amounts in the sub-nanoliter range was presented. Within this work, the potential of single drop analyses in comparison to conventional systems based on nebulizers should be demonstrated. Compared to other systems, which also allow a low-loss analysis of small sample volumes, the above system features advantages like a modulated or pulsed introduction, respectively. In combination with separation methods such as nano-HPLC, this method could represent an important step forward in the field of the analysis of smallest sample amounts. In general, the principle of a piezoacoustic droplet generation should be suitable for a coupling with such separation techniques. For that purpose, however, additional

(15) Hohreiter, V.; Hahn, D. W. *Anal. Chem.* **2006**, *78*, 1509.

(16) Diwakar, P. K.; Jackson, P. B.; Hahn, D. W. *Spectrochim. Acta, Part B* **2007**, *62*, 1474.

developmental efforts in the fields of microfluidics and microfabrication are necessary. For example, drawbacks of the commercial droplet generator that was used for the current measurements, namely, a large dead volume, have to be surmounted. With the relatively large liquid reservoir set aside together with the tubing, the dead volume can be reduced to the inner volume of the capillary, which is estimated at 50 nL. Further reduction of the minimal amount of liquid that can be analyzed without prior dilution might be achieved by employing advanced microfluidic technologies. In consideration of such modifications in a lab-on-a-chip environment, the MDMD system might outperform nebulizers when the microfluidic chip is hyphenated to a detection system like ICPMS. Nebulizers cause issues due to incompatibilities of analyte liquid flow rates, which were the object of investigation.¹⁷ Thus the drawback of a small detection limit in absolute terms when dealing with a limited sample amount does not apply for the use of monodisperse microdroplets for analytical purpose.

The proof of applicability and the relatively good detection limits were achieved using LIBS and ICP-OES. In the case of ICP spectrometry, the step toward ICP mass spectrometry would allow lowering the detection limits by 2–3 orders of magnitude. Concurrently, LIBS-based microdroplet analysis appears to be the method of choice when a simple and low-priced tool for the analysis of the smallest sample amounts is required.

The Ca detection limit obtained in this study for the LIBS system was comparable or better than other LIBS studies on the aqueous and single droplet analyte. The absolute detection limit obtained in this study corresponds to an absolute mass of 0.5 and 23 fg (3.3 fg when averaging) of Ca per droplet for ICP and LIBS, respectively, which is well-suited for analytical studies where

absolute mass detection is more critical but the availability of the analyte sample is limited. When directly comparing the two analytical methods, the relative detection limit is low for the LIBS system as compared with the ICP-OES system, although the analytical performance should be considered in the context of the specific application, while the robustness and simplicity of the LIBS method should also be considered. In summary, sample introduction into these two analytical plasmas by MDMD shows great potential for efficiently introducing very small analyte volumes into the plasma. When appropriately engineered into sensing platforms to reduce sample dead volumes, this technology may have great implications for ultralow sample volume applications, for example, nano-HPLC and lab-on-the-chip applications, as well as other plasma-based analytical schemes.

ACKNOWLEDGMENT

The Plasma-Analyte Interaction Working Group (PAIWG) is a collaborative effort of the University of Florida (USA), the Federal Institute of Material Research and Testing (BAM) in Berlin (Germany), and ISAS-Institute for Analytical Sciences in Dortmund (Germany), jointly funded by NSF (Grant No. CHE-0822469) and DFG. The authors gratefully acknowledge financial support by the National Science Foundation (Grant CHE-0822469) and the Deutsche Forschungsgemeinschaft (Grant NI 185/38-1) through the jointly funded research project “Solving the plasma analyte interaction problem: Towards a fundamental advancement in plasma-assisted microanalysis and material characterization.”

Received for review August 31, 2009. Accepted January 28, 2010.

AC901966Z

(17) Pearson, G.; Greenway, G. *J. Anal. At. Spectrom.* **2007**, *22*, 657.